

## CHARACTERIZATION OF MICROSTRUCTURAL ANISOTROPY OF STEELS BY MEANS OF MATHEMATICAL MORPHOLOGY

Horst Wendrock, Roland Hübel

Institut für Festkörper- und Werkstofforschung e.V.  
01171 Dresden, Germany

### ABSTRACT

The covariance and the contact distribution function are measured to quantify microstructural anisotropies in hot-rolled ferritic-pearlitic steels. A quantity for the degree of pearlite banding is derived from the differences found in linear contact distributions, measured in longitudinal and transversal direction. To have an "isotropic case" for comparison, a Boolean model is adapted to the measured basic parameters  $V_V$  and  $S_V$ , and its contact distribution is evaluated.

**Key words:** anisotropy, Boolean model, contact distribution, covariance, steel.

### INTRODUCTION

Anisotropies in microstructure of metallic materials often have an essential influence on mechanical properties. In high-strength steels the fracture toughness of hot rolled plates is decreased when banding of pearlite phase occurs. To optimize the technology (heat treatment, rolling conditions etc.) of such materials, quantification of this kind of anisotropy is necessary. Some recent attempts to do this are known (Saltykov, 1974; Kugler et al., 1991), but they only give integral information on orientation of the phase surfaces or need some empirical assumption about materials behaviour for their preprocessing steps.

In the present paper a method is proposed to characterize the degree of banding in microstructures objectively without empirical assumptions by help of procedures from Mathematical Morphology. The covariance and the linear contact distribution function both in longitudinal and transversal direction were measured to derive width and distance of bands and a quantity which describes the degree of banding.

### MATERIALS AND METHODS

For demonstration two low alloyed-HS-steel samples from controlled rolled plates of 30 mm thickness have been chosen, one (sample A) being normalized after rolling in order to minimize banding effects. Metallographic cross sections of the steel samples were etched chemically so that the pearlite phase appears dark and also the boundaries of ferrite grains are visible. In Fig. 1 the difference between sample A and B in the arrangement of the pearlite regions are shown. The analysis of the pearlite regions was done by an image analyser Q 570 on images from light microscope (magnification at about 800x). In every measurement 20 images of 512<sup>2</sup> pixels (pixel length nearly 0.5  $\mu\text{m}$ ) were measured and accumulated.

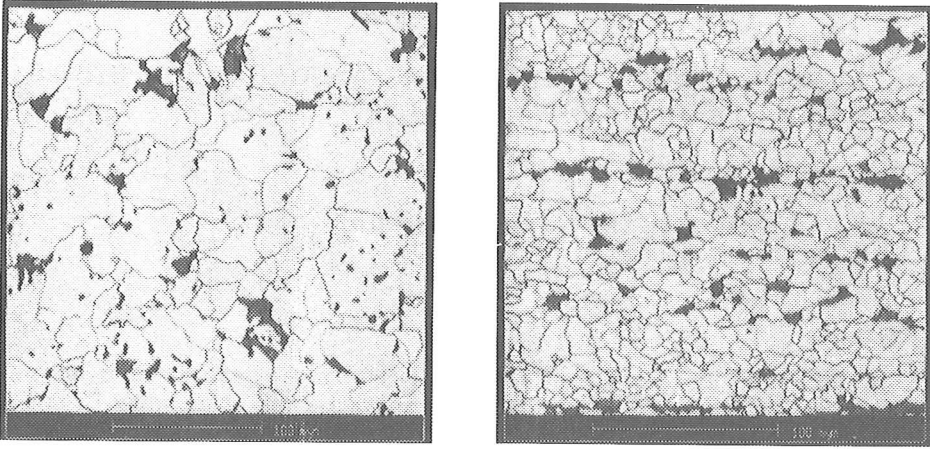


**Fig.1.** Microstructure of the steels under investigation, sample A (left) and B (right).

Before the measurements some image enhancement was performed (eliminating of little etching artifacts, separating and reconstructing ferrite grain boundaries) and after that the pearlite areas were detected. Afterwards the basic parameters of microstructure (volume fraction and surface density) were evaluated by field specific measurement.

#### Measurement of covariance

By definition the covariance of the set  $X$  is the probability, that two points with distance  $r$  both lie in  $X$  (Fig. 2):

$$C(X; r, \alpha) = p(x \in X, (x + \vec{r}) \in X). \quad (1)$$

Edge corrected estimation of the covariance in a window  $W$  was achieved by cyclic shifting of the image and measuring the area fraction of the shifted image masked by the original one in the window linearly eroded with  $r$  (Stoyan et al., 1987):

$$C(r) = \frac{A[(X \cap X_r) \cap (W \cap W_r)]}{A(W \cap W_r)}. \quad (2)$$

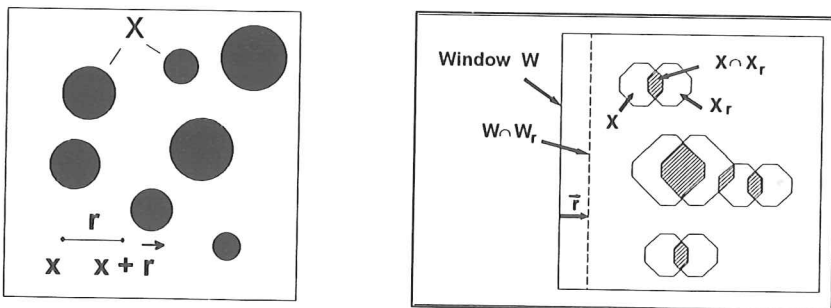


Fig. 2. Definition and measurement of the covariance.

From the transversally measured covariance the first local minimum and maximum were derived (if they existed) to give a mean value for width and distance of pearlite bands.

**Measurement of contact distribution function (CDF)**

By definition, the CDF is connected with the conditional probability that a disk with radius (line with length)  $r$  is lying completely in  $X^C$ , given that the centre of the disk (end of the line) does not belong to  $X$ . Edge corrected estimation of the CDF in a window  $W$  can be achieved by cyclic erosion of the complement and by measurement of the area fraction in the window frame eroded in the same manner (Stoyan et al., 1987):

$$H_B(r) = 1 - \frac{A_A[(X^C \ominus r B) \cap (W \ominus r B)]}{A_A[(X^C) \cap (W \ominus r B)]} \quad (3)$$

where  $B$  is a disk with radius 1 or a line with length 1 for spherical or linear CDF, respectively (Fig. 3).

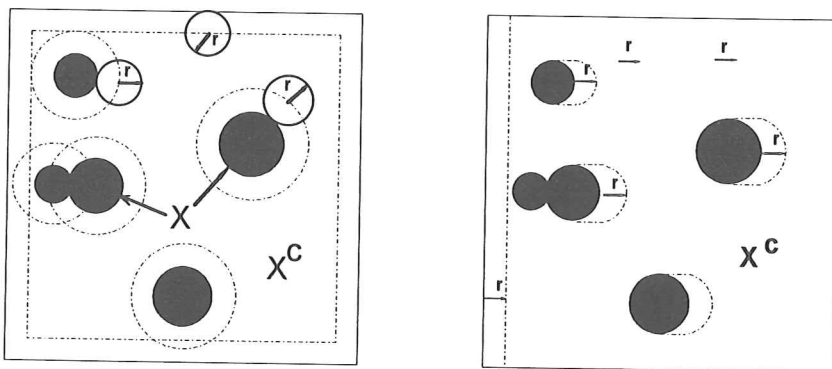


Fig. 3. Definition and measurement of the spherical (left) and linear (right) contact distribution function.

### The isotropic case - Boolean model

As a model for random and isotropic arrangement the well-known Boolean model was chosen. For this model, a series of relations between the model parameters (primary grain intensity,  $\lambda_A$ , mean grain area,  $\bar{A}$ , and mean grain perimeter,  $\bar{U}$ ) and the measurable parameters (area fraction,  $A_A$ , boundary length per unit area,  $L_A$ , and specific convexity number,  $N_A^+$ ) is known:

$$A_A = 1 - \exp(-\lambda_A \bar{A}), \quad (4)$$

$$L_A = \lambda_A (1 - A_A) \bar{U}, \quad (5)$$

$$N_A^+ = \lambda_A (1 - A_A). \quad (6)$$

For a given set of basic parameters, the parameters of Boolean model can be estimated with Eqs. 4 to 6. Furthermore, for convex grains the model yields for the linear and spherical CDF:

$$H_L(r) = 1 - \exp(-\lambda_A \bar{U} r / \pi), \quad (7)$$

$$H_S(r) = 1 - \exp(-\lambda_A \bar{U} r - \pi \lambda_A r^2). \quad (8)$$

These functions can be linearized, and the quantile  $R_\gamma$  can be obtained:

$$\ln(1 - H_L(r)) = -r \frac{L_A}{\pi(1 - A_A)} \quad (9)$$

$$R_\gamma(H_L) = -\ln(1 - \gamma) \frac{\pi(1 - A_A)}{L_A}. \quad (10)$$

These formulae show how for a Boolean model the linear CDF depends on  $A_A$  and  $L_A$ . They can therefore be used for normalization of the  $R_{0.5}$  - quantiles measured in the real structure.

For the characterization of banding the spherical and linear CDF's of pearlite were measured. We defined the degree of banding  $\varepsilon$  as the absolute difference of the 50 %-quantiles of the linear CDF parallel and transversal to the rolling direction, divided by the 50 %-quantile of the linear CDF of the adapted isotropic (Boolean) model evaluated from the basic parameters  $A_A$  and  $L_A$  with Eq. 10:

$$\varepsilon = \frac{|R_{0.5}(x) - R_{0.5}(y)|}{R_{0.5}^{(BM)}}. \quad (11)$$

For comparison, the degree of orientation of the 50 %-quantiles of the linear CDF's, Eq. 12, and of the mean chord lengths, Eq. 13, was calculated:

$$\alpha_1 = \frac{|R_{0.5}(x) - R_{0.5}(y)|}{R_{0.5}(x) + R_{0.5}(y)} * 100\%, \quad (12)$$

$$\alpha_2 = \frac{|\bar{l}(x) - \bar{l}(y)|}{\bar{l}(x) + \bar{l}(y)} * 100\%. \quad (13)$$

**RESULTS**

For the two samples shown in Fig. 1, the basic parameters of microstructure were determined. The values of volume fraction and surface density in Table 1 are nearly equal, only the mean chord lengths of sample B in X- and Y-direction are different.

**Table 1.** Measured basic parameters of the pearlite phase.

Parameter/ Sample		sample A	sample B
volume fraction	(%)	$5.7 \pm 0.9$	$5.5 \pm 1.1$
surface density	( $\text{mm}^{-1}$ )	41.6	40.1
mean chord length in X-direction	( $\mu\text{m}$ )	5.99	6.58
mean chord length in Y-direction	( $\mu\text{m}$ )	5.72	4.97

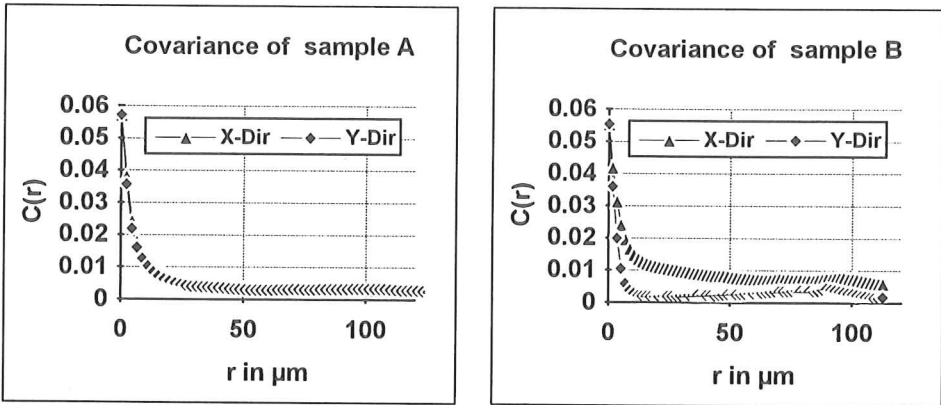


**Fig. 4.** Measured covariance of the pearlite phase.

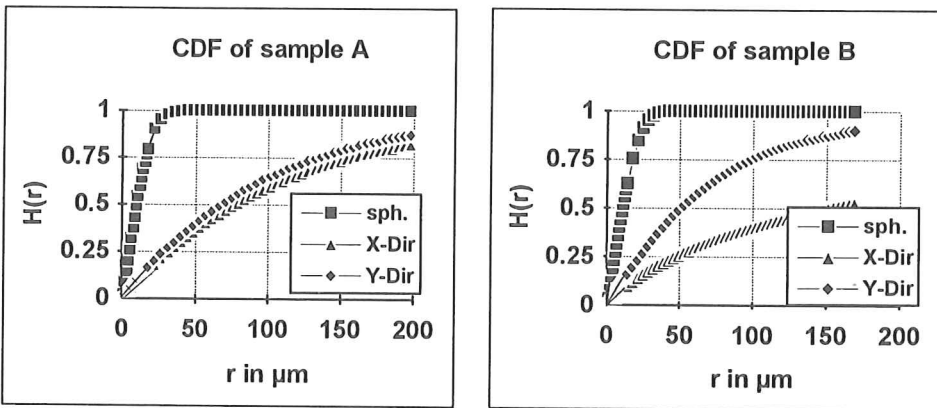


**Fig. 5.** Measured spherical and linear contact distribution functions of the pearlite phase.

The measured covariances (Fig. 4) reveal distinct differences between both directions in sample B. In X-direction the function falls very slowly to the asymptotic value and in Y-direction the function has a periodicity. The linear CDF's of sample B (Fig. 5) have also different ascents and consequently different  $R_{0.5}$  - quantiles. The degree of orientation  $\alpha_1$  (6.4 and 49.7 %) derived from the  $R_{0.5}$  - quantiles is larger than the degree of orientation  $\alpha_2$  (2.3 and 13.9 %) derived from the chord lengths. The degree of banding  $\epsilon$  shows also considerable differences between samples A and B.

**Table 2.** Measured anisotropy of the pearlite phase.

Parameter/ Sample		sample A	sample B
mean width of bands	( $\mu\text{m}$ )	-	22
mean distance of bands	( $\mu\text{m}$ )	-	90
$R_{0.5}$ of $H_L(r)$ in X-direction	( $\mu\text{m}$ )	76.6	150.6
$R_{0.5}$ of $H_L(r)$ in Y-direction	( $\mu\text{m}$ )	67.3	50.6
$R_{0.5}^{(BM)}$ of adapted model	( $\mu\text{m}$ )	62.8	65.2
degree of banding $\epsilon$		0.147	1.534
degree of orientation $\alpha_1$	(%)	6.4	49.7
degree of orientation $\alpha_2$	(%)	2.3	13.9

## DISCUSSION

The suggested degree of banding  $\epsilon$  and of orientation  $\alpha_1$  indicate anisotropy effects very distinctively and with good statistical significance. In future, more work shall be done to apply the methods described here for optimizing steel technology.

## REFERENCES

- Kawalla R, Kugler J, Lotter U. Beispiele zur Anwendung der automatischen Bildanalyse in der Werkstofftechnik. In: Sonderband Prakt Metallographie 1992; 24 : 293-302.
- Ohser J, Tscherny H. Grundlagen der quantitativen Gefügeanalyse, Freiburger Forschungshefte 1988; B 264: 28-45
- Saltykov S A. Stereometrische Metallographie. Leipzig: Grundstoffverlag, 1974:155-193.
- Serra J. Image Analysis and Mathematical Morphology. London: Academic Press, 1982: 271-297.
- Stoyan D, Kendall W, Mecke J. Stochastic Geometry and its Applications. Berlin: Akademie Verlag, 1987.